DOI: 10.1002/cbic.200800165

Smart Magnetic Resonance Imaging Agents that Sense Extracellular Calcium Fluctuations

Goran Angelovski,*[a] Petra Fouskova,[b] Ilgar Mamedov,[a] Santiago Canals,[a] Eva Toth,*[b] and Nikos K. Logothetis[a, c]

Understanding brain function requires not only a comprehension of the physiological workings of its individual elements, that is, its neurons and glia cells, but also demands a detailed map of its functional architecture and a description of the connections between populations of neurons, the networks that underlie behaviour. Microelectrode recordings yield information only about single neurons. The activity of networks can be better studied with in vivo neuroimaging, such as positron emission tomography (PET) and magnetic resonance imaging (MRI). The so-called blood-oxygen-level-dependent (BOLD) functional MRI (fMRI) is today the mainstay of volume neuroimaging in humans and animals. It capitalises on the neuro–metabolic and neuro–vascular link; in other words, it exploits the increases in metabolism and blood flow that ensure a regional brain activation.[1,2]

However, the BOLD technique has unavoidable physiological limitations that are derived from the very vascular origin of the signal, which reduces the maximal achievable temporal resolution to several seconds and complicates its functional interpretation. Despite recent advances in the understanding of the neurophysiological basis of fMRI signals,[3] the relationship between the measured BOLD signal and the underlying neural activity is still not well understood.[1,2] Thus, the use of other MRI techniques based on paramagnetic contrast media, such as complexes of gadolinium,[4,5] seems to be mandatory, and the involvement of synthetic, coordination and physical chemistry might have an important contribution to overcoming some of the current problems.

A step forward in the fMRI field is the development of bioactivated, responsive or "smart" contrast agents (SCA) as functional markers for signals that are directly linked to neuronal processing, thus resulting in a fMRI signal that is independent of neurovascular coupling and the obligatory slow haemodynamic responses.[6] "Intelligent" probes that involve pH-sensitive,[7–9] metal-ion-activated,[10–16] enzyme-activated[17–19] or oxygen-activated[20] metal complexes have slowly been developed. For tracking neural activity, several possible markers that are responsive to the concentration of certain ions, neurotransmitters or transmembrane potential might be envisaged. Very important work in this direction has been performed in recent years by imaging fluorescence signals that report intracellular Ca^{2+} fluctuations.[21–23] Ca^{2+} ions are indeed crucial in several steps in neuronal signalling, and their intra- and extracellular concentrations change dramatically during brain activity.[24]

Attempts toward Ca^{2+}-sensitive MRI SCA that mainly use two different approaches have been reported: 1) DOPTA–Gd has a T_1 response upon interaction with Ca^{2+} ions,[10] 2) a T_2 agent that is based on the Ca^{2+}-related aggregation of superparamagnetic iron nanoparticles and calmoduline.[11] Both approaches have limitations. Given its dissociation constant in the μM range, DOPTA–Gd is not capable of reporting Ca^{2+} concentration changes in the extracellular space (mM range). In addition, due to the low sensitivity of MRI, DOPTA–Gd can hardly detect changes in intracellular Ca^{2+}. On the other hand, the time course of the Ca^{2+}-dependent aggregation of superparamagnetic iron oxide (SPIO) conjugates is above 1 s, which prevents the tracking of fast Ca^{2+}-concentration changes. Thus, the development of novel smart MR agents that are able to sense and report physiological Ca^{2+} fluctuations is desirable.

In an attempt to circumvent current problems and the lack of an efficient Ca^{2+} MR marker, we have designed complexes **Gd_2L^1** and **Gd_2L^2** (Scheme 1), which are expected to promptly respond to a Ca^{2+}-concentration change by altering their magnetic properties. We considered that a T_1 agent (Gd^{3+} complex) would be more favourable, because a fast magnetic response can be achieved only by intramolecular interactions.[25] Also, to detect MRI contrast changes that are related to the relaxivity change of a SCA upon interaction with Ca^{2+}, one needs relatively high concentrations of the agent, and the conditional dissociation constant of the Ca^{2+}–SCA entity should be in the mM range under physiological conditions. Thus, targeting the extracellular Ca^{2+} seems more reasonable, given that the concentration of free extracellular Ca^{2+} can decrease up to 30% from its resting state (~1.2 mM) during intense stimulation.[24,26] Furthermore, targeting extracellular Ca^{2+} mitigates the chemical design, because additional requirements for cell internalisation can be neglected.

The ligand of choice was a modified EGTA chelator linked to two macrocyclic moieties that bear Gd^{3+} ions. EGTA is highly selective for Ca^{2+} ($\log K_{CaEGTA} = 11.0$ vs. $\log K_{MgEGTA} = 5.2$).[27] As we recently described, the transformation of carboxylate

[a] Dr. G. Angelovski, Dr. I. Mamedov, Dr. S. Canals, Prof. Dr. N. K. Logothetis
Abteilung Physiologie Kognitiver Prozesse
Max-Planck-Institut für Biologische Kybernetik
Spemannstrasse 38, 72076 Tübingen (Germany)
Fax: (+49) 7071-601-919
E-mail: goran.angelovski@tuebingen.mpg.de

[b] Dr. P. Fouskova, Dr. E. Toth
Centre de Biophysique Moléculaire, CNRS
rue Charles Sadron, 45071 Orléans, Cedex 2 (France)
Fax: (+33) 2-38-63-15-17
E-mail: eva.jakabtoth@cnrs-orleans.fr

[c] Prof. Dr. N. K. Logothetis
Imaging Science and Biomedical Engineering
University of Manchester, Oxford Road
M13 9PT, Manchester (UK)

Supporting information for this article is available on the WWW under http://www.chembiochem.org or from the author.

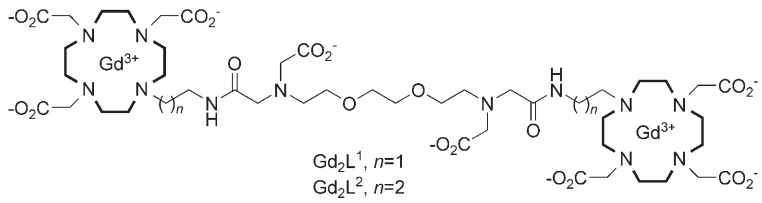

Scheme 1. Structures of investigated complexes $\mathbf{Gd_2L^1}$ and $\mathbf{Gd_2L^2}$.

groups of poly(amino carboxylates) into amides leads to a decrease in the Ca^{2+}-association constant by several $\log K$ units, while the selectivity for Ca^{2+} versus other competitive metals, mainly Mg^{2+}, is preserved. Furthermore, the high flexibility of the Ca^{2+}-complexing unit also seems to be beneficial.[28,29]

The facile synthesis of the desired products was performed by considering their complex structure and limited freedom for undergoing several synthetic transformations with quite massive and acid-sensitive reagents, such as DO3A–*t*Bu-ester derivatives (Scheme 2). Namely, the protected amine **1**, which underwent alkylation of *tert*-butyl 2-bromoacetate and reductive removal of two benzyl groups, gave precursor **3**. The second precursor for coupling was obtained in a single reaction step by an amide formation from DO3A–ethylamine/DO3A–propylamine and 2-bromoacetic acid. In the next step, the secondary bis-amine **3** was alkylated with bromides **5a**,**b** to give bis-macrocycles **6a**,**b** in good yields. Deprotection of the *tert*-butyl groups in both bis-macrocycles yielded the final ligands $\mathbf{L^1}$ and $\mathbf{L^2}$, which after complexation with Gd^{3+} in water under neutral pH gave $\mathbf{Gd_2L^1}$ and $\mathbf{Gd_2L^2}$.

The influence of Ca^{2+} on the paramagnetic properties of the Gd^{3+} complexes was investigated by relaxometric titrations (11.75 T, 25 °C, in HEPES buffer; Figure 1). After the addition Ca^{2+} (5–6 equiv), the initial relaxivities of 4.05 and 3.44 $mM^{-1}s^{-1}$ for $\mathbf{Gd_2L^1}$ and $\mathbf{Gd_2L^2}$, respectively, reached the maximal values of 6.86 and 6.29 $mM^{-1}s^{-1}$ (69 and 83% relaxivity increase for $\mathbf{Gd_2L^1}$ and $\mathbf{Gd_2L^2}$, respectively). The fitting of the curves resulted in the apparent association constants of $\log K_A = 3.7 \pm 0.2$ ($\mathbf{Gd_2L^1}$) and $\log K_A = 4.7 \pm 0.3$ ($\mathbf{Gd_2L^2}$). The reversibility of the SCA–Ca^{2+} interaction was checked by the addition of an equimolar amount of EDTA with respect to the Ca^{2+}. For both complexes, the relaxivity dropped back to the values of the Ca^{2+}-free solutions. Both complexes are highly selective toward Ca^{2+} versus Mg^{2+}, which are the only physiologically abundant alkaline earth cations. The total relaxivity change after the addition of ~5 equivalents of Mg^{2+} was 3 and 6% for $\mathbf{Gd_2L^1}$ and $\mathbf{Gd_2L^2}$, respectively. Accordingly, when Ca^{2+} (~5 equiv) was added to solutions that already contained Mg^{2+}, the relaxivity of the complexes reached the plateau as in the Mg^{2+}-free experiments.

The mechanism responsible for the relaxivity change upon the SCA–Ca^{2+} interaction was previously investigated for similar systems.[13,16,28,29] The contribution of the rotational dynamics to the overall relaxivity is minimised at high magnetic fields,[30] and the water-exchange rate, which could change upon addition of Ca^{2+}, does not affect the relaxivity. Consequently, the main parameter that determines relaxivity is the inner-sphere hydration number. Indeed, a q assessment was performed on Eu^{3+} analogues $\mathbf{Eu_2L^1}$ and $\mathbf{Eu_2L^2}$ by means of time-resolved luminescence decay measurements. Estimated values of q change upon addition of one equivalent of Ca^{2+} from 0.3 to 0.7 and 0.5 to 0.9 for $\mathbf{Eu_2L^1}$ and $\mathbf{Eu_2L^2}$, respectively; this confirms that the observed relaxivity changes are induced by an increase of the inner-sphere hydration number of the investigated complexes.

The potential of MR probes were further investigated in more complex solutions that mimic the extracellular brain fluid. We applied a 1:1 mixture of the Dulbecco's modified Eagle's medium (DMEM, Ca^{2+}-free) and Ham's F-12 nutrient mixture (F-12), which are widely used media for the culture of neurons and other cell types.[31] A residual amount of Ca^{2+} (0.299 mM) is present in the F-12 solution, along with other cations (Na^+, K^+, Mg^{2+}, Fe^{2+}/Fe^{3+}, Zn^{2+}), anions (Cl^-, SO_4^{2-},

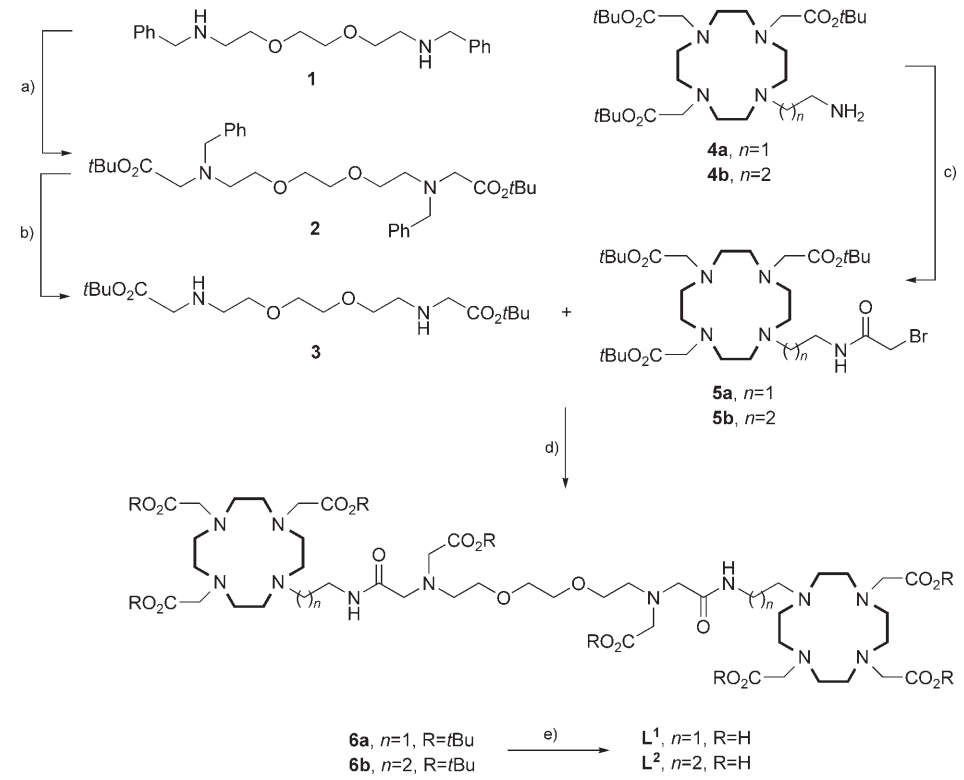

Scheme 2. Synthesis of $\mathbf{L^1}$ and $\mathbf{L^2}$. Reagents and conditions: A) $BrCH_2CO_2tBu$, K_2CO_3, CH_3CN, 80 °C; B) H_2, 10% Pd/C, CH_3OH; C) $BrCH_2CO_2H$, DCC, DMAP (cat.), CH_2Cl_2; D) K_2CO_3, CH_3CN, 80 °C; E) HCO_2H, 60 °C.

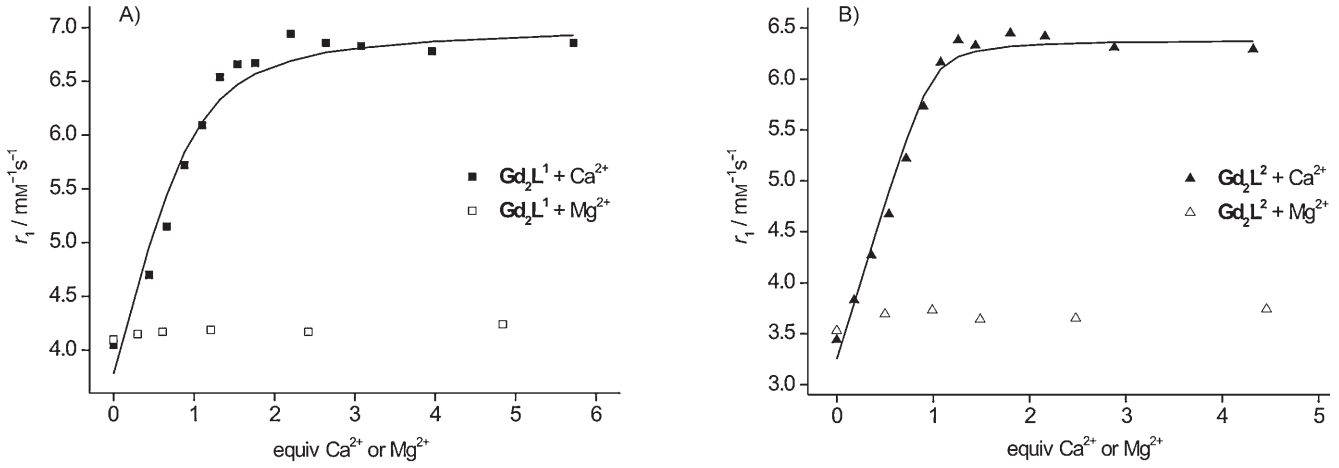

Figure 1. Relaxometric Ca^{2+} and Mg^{2+} titrations in the buffer solutions. Relaxometric titrations of A) $\mathbf{Gd_2L^1}$ and B) $\mathbf{Gd_2L^2}$ with Ca^{2+} (full symbols) and Mg^{2+} (open symbols) at 11.75 T, 25 °C, pH 7.3 (HEPES). The lines correspond to the fit that is described in the Experimental Section [Eq. (2)].

HCO_3^-, $HPO_4^{2-}/H_2PO_4^-$) and amino acids in physiological concentrations. The relaxometric Ca^{2+} titrations that were performed at 37 °C resulted in an overall relaxivity change of 39 and 37% for $\mathbf{Gd_2L^1}$ and $\mathbf{Gd_2L^2}$, respectively (Figure 2). The absolute relaxivities are smaller in this complex medium at 37 °C than in water at 25 °C. On the other hand, we cannot exclude

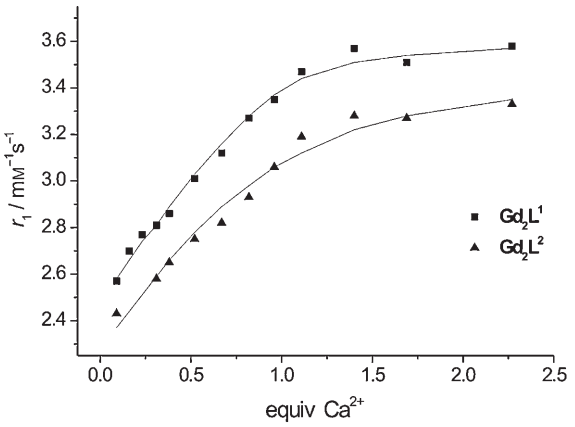

Figure 2. Relaxometric Ca^{2+} titration curves of $\mathbf{Gd_2L^1}$ (■) and $\mathbf{Gd_2L^2}$ (▲) in DMEM/F-12, 1:1 (*v/v*) were performed at 37 °C, pH 7.3 (25 mM HEPES) and 11.75 T. The lines correspond to the fit described in the Experimental Section [Eq. (2)].

that some anion binding, which is common for DO3A and its derivatives could also contribute to the diminution of the hydration number and thus the relaxivity.[32,33] The apparent association constants that were obtained from the fit of the titration curves are $\log K_A = 4.1 \pm 0.2$ and $\log K_A = 3.5 \pm 0.2$ for $\mathbf{Gd_2L^1}$ and $\mathbf{Gd_2L^2}$, respectively. The reversibility of SCA–Ca^{2+} interaction was confirmed again by EDTA addition.

To further simulate the biochemical complexity of the brain and investigate the Ca^{2+}-sensing properties of our complexes in a biologically more realistic environment, we performed Ca^{2+} titrations in the DMEM/F-12 medium that contained GIBCO™ N-2 supplement (N-2). N-2 is composed of a mixture of proteins (human transferrin and insulin) and hormones (progesterone) with trace amounts of putrescine. We consider the DMEM/F-12/N-2 mixture to be a very good approximation of the brain extracellular medium (BEM). Upon addition of 1.6–1.8 equiv Ca^{2+}, the relaxivity of $\mathbf{Gd_2L^1}$ increased from 2.61 to 3.94 mM^{-1}s^{-1} whereas for $\mathbf{Gd_2L^2}$ it increased from 2.46 to 3.73 mM^{-1}s^{-1} (51 and 52% change, respectively), and the fitted apparent association constants were $\log K_A = 4.3 \pm 0.3$ and $\log K_A = 4.6 \pm 0.4$, for $\mathbf{Gd_2L^1}$ and $\mathbf{Gd_2L^2}$, respectively. To simulate the transient nature of the Ca^{2+} changes during neural activity, a subsequent "reverse" titration with EDTA was performed, so that the relaxivities returned to the initial values; this confirmed the reversibility of the Ca^{2+}–contrast agent interaction even in a complex environment (Figure 3).

The maximal change in Ca^{2+} concentration that might be expected in the brain is in the range of 0.8–1.2 mM. To estimate the free Ca^{2+} concentration that is effectively available to interact with the Gd^{3+} complex in the BEM and thus correct the concentration axis in Figure 3 (total Ca^{2+} concentration) with the Ca^{2+} quantity that might be involved in protein binding, we carried out potentiometric titrations using a Ca^{2+}-selective electrode. Experiments were performed under identical conditions (temperature, BEM cocktail and Ca^{2+}-stock solutions) as in the analogous relaxometric titrations. In both cases (DMEM/F-12 without and with N-2), the slopes of the electromotive force versus $\log[Ca^{2+}]$ curves differ by less than 2–3 mV from the theoretical Nernst value (30.77 mV). In addition, the free Ca^{2+} concentration was determined with the standard addition method (Gran plot[34]) and no remarkable Ca^{2+} sequestration was observed; this excludes any significant Ca^{2+} chelation by proteins or any other component of the medium (Figure 4). Therefore, the concentrations of total Ca^{2+} used in all titration experiments were considered as "free/available" Ca^{2+} concentrations in the fitting of the relaxivity titration curves.

The results that were obtained in the BEM model are extremely encouraging and the in vivo characterisation of the complexes is in progress. $\mathbf{Gd_2L^1}$ and $\mathbf{Gd_2L^2}$ are still active and

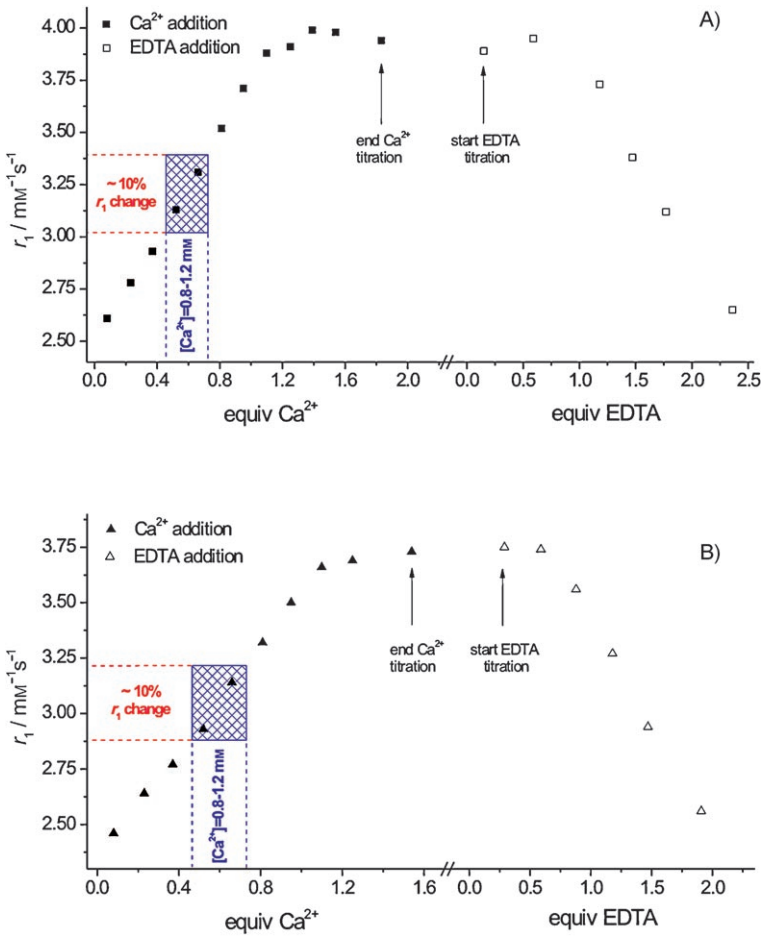

Figure 3. Relaxometric titrations of A) Gd_2L^1 and B) Gd_2L^2 with Ca^{2+} (full symbols) and EDTA (open symbols) in BEM at 11.75 T, 37 °C, pH 7.3 (25 mM HEPES).

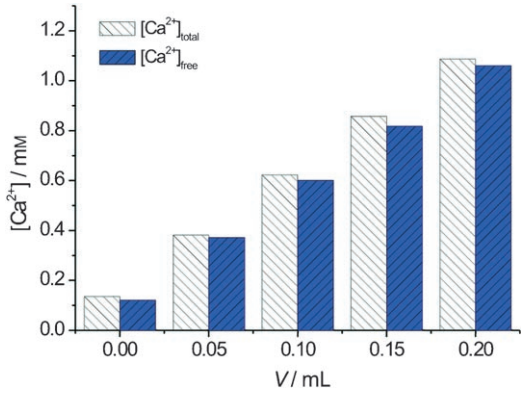

Figure 4. Total Ca^{2+} concentration in BEM compared to the free Ca^{2+} concentration, which was determined by the standard addition method.

sensitive to Ca^{2+} concentration changes in the medium that bears a resemblance to the brain extracellular fluid. Moreover, the relaxivity changes are as high as ~10% in the relevant range of Ca^{2+} modulation in the brain (0.8–1.2 mM, Figure 3). Previous theoretical studies predict that ~5% signal change is detectable in a time-resolved experiment.[25] Therefore, these complexes possess great application potential as fast responding smart contrast agents.

In this work we report the synthesis and characterisation of two novel Gd^{3+} complexes that exhibit a remarkable relaxivity response with high selectivity and full reversibility in their interaction with Ca^{2+}. Given the structural complexity, the synthesis of complexes is quite facile and provides the desired structures in satisfactory yields. Moreover, this straightforward procedure enables further structural improvements of the chelates. Physicochemical characterisation of both complexes emphasised the high relaxivity changes upon alteration of the Ca^{2+} concentration. Their behaviour in a biologically relevant medium, such as the model of the brain extracellular fluid, is extremely promising. Because they are able to alter their magnetic properties in response to Ca^{2+}-concentrations changes, these molecules have great potential to function also in real in vivo conditions. This can be exploited to track in vivo changes of extracellular Ca^{2+} flux, and thus, neural activity. Through their remarkable relaxivity properties, these complexes could lead to high-resolution MR imaging of brain function.

Experimental Section

Materials: 1,2-Bis(2-benzylaminoethoxy)ethane was purchased from TCI Europe (Zwijndrecht, Belgium). Cyclen was purchased from Strem (Bischheim, France). All other chemicals were purchased from Sigma–Aldrich or Acros Organics and were used without further purification. DO3A–*t*Bu-ester, DO3A-ethylamine (DO3A–EA, **4a**) and DO3A–propylamine (DO3A–PA, **4b**) were synthesised according to previously reported procedure; DO3A is 1,4,7,10-tetraazacyclododecane-1,4,7-triacetic acid.[28] Column chromatography was performed by using silica gel 60 (70–230 mesh ASTM) from Merck. DMEM (without L-glutamine, sodium pyruvate and calcium chloride; catalogue number: 21068028), Ham's F-12 nutrient mixture (catalogue number: 21765029) and N-2 supplement (catalogue number: 17502048) were purchased from Invitrogen.

Instruments: ^{1}H NMR and $^{13}C\{^1H\}$ NMR spectra were recorded by using a Bruker DRX400 spectrometer at room temperature. Relaxometric experiments were performed on a Bruker Avance 500 spectrometer. ESI-HRMS were performed by using a Bruker BioApex II ESI-FT-ICR, that was equipped with an Agilent ESI-source, measured by flow injection analysis. ESI-LRMS were performed by using an ion trap SL 1100 system (Agilent). Size exclusion chromatography was performed with Amersham ÄKTA purifier by using HiLoad 26/60 Superdex 30 column from GE Healthcare Biosciences. Luminescence lifetime measurements were performed by using QuantaMaster™ 3-PH fluorescence spectrometer from Photon Technology International, Inc., (Monmouth Junction, NJ, USA). Potentiometric titrations were performed by using Metrohm Basic Titrino 794 (Herisau, Switzerland), with calcium-selective (ELIT 8041) and AgCl reference (ELIT 001n) electrodes that were purchased from NICO2000 Ltd. (Middlesex, UK).

Synthesis: Compounds **2**, **3**, **5a**, **5b**, **6a**, **6b**, L^1 and L^2 were synthesised by following the synthetic pathway that is described in

Scheme 2. Detailed synthetic procedures and spectroscopic data are available in the Supporting Information.

Relaxometric Ca^{2+}, Mg^{2+} or EDTA titrations of Gd_2L^1 and Gd_2L^2: The titrations were performed at 11.75 T, 25 °C or 37 °C and pH 7.3–7.4 (maintained by HEPES buffer). A solution of $CaCl_2$, $MgCl_2$ or EDTA of known concentration was added stepwise to the complex solution and the longitudinal proton relaxation time T_1 was measured after each addition of the analyte. The relaxivity r_1 was calculated from Equation (1) by using the actual Gd^{3+} concentration at each point of the titration. The initial Gd^{3+} concentrations were determined by measuring the bulk magnetic susceptibility shifts.[35]

$$\frac{1}{T_{1,obs}} = \frac{1}{T_{1,d}} + r_1[\mathrm{Gd}] \quad (1)$$

where $T_{1,obs}$ is the observed longitudinal relaxation time, $T_{1,d}$ is the diamagnetic contribution in the absence of the paramagnetic substance and [Gd] is the concentration of Gd^{3+}. The titration curves were fitted to Equation (2) to obtain the apparent association constants, which should be compared with the conditional stability constant, $\log K_{cond}$, of Ca–EGTA at pH 7.4, calculated by taking into account the protonation constants of $EGTA^{4-}$.

$$r_1^{obs} = r_1^{min} + (r_1^{max} - r_1^{min}) \times \frac{(K_A \times c_{Gd_2L} + K_A \times c_{Ca} + 1) - \sqrt{(K_A \times c_{Gd_2L} + K_A \times c_{Ca} + 1)^2 - 4K_A^2 \times c_{Gd_2L} \times c_{Ca}}}{2 \times c_{Gd_2L} \times K_A} \quad (2)$$

Luminescence lifetime experiments: The decay experiments were performed on $\mathbf{Eu_2L^1}$ and $\mathbf{Eu_2L^2}$ (2.5 mM, 25 °C, pH 7.3) in H_2O and D_2O. The Eu^{3+} ion was directly excited at 395 nm and emission intensity at 615 nm was recorded with 10 μs resolution. Excitation and emission slits were set to 15 and 5 nm bandpass, respectively. Datasets were averages of 25 scans and each reported value is the mean of three independent measurements. Obtained curves were fitted to the first-order exponential decay with $r^2 = 0.99$. The q values were calculated from Equation (3) (Table S11).[36] Upon addition of the second equivalent of Ca^{2+}, no change in q was observed.

$$q = 1.2 \times (\tau_{H_2O}^{-1} - \tau_{D_2O}^{-1} - 0.25) \quad (3)$$

Potentiometric titrations: Calibration experiments were performed in DMEM/F-12 1:1 (*v*/*v*) by adding 50 μL increments of a 10.017 mM Ca^{2+} stock solution (Figure S1). According to the manufacturer's specifications, Ca^{2+} chelator was not present in either DMEM or F-12 media. The starting Ca^{2+} concentration was $[Ca^{2+}] = 0.1495$ mM. Slopes were obtained from the linear fit by using the Nernst equation:[34]

$$E = K + S \log [Ca^{2+}] \quad (4)$$

where E is the measured potential, K is the electrode constant, S is the slope, $S = 2.303\ RT/zF$, $R = 8.314\ J K^{-1} mol^{-1}$, $F = 96\,480\ C mol^{-1}$, $T = 310$ K. Obtained results were an average of three titrations; determined slope: $S = 28.39$ mV.

Titrations with BEM: Titrations with DMEM/F-12/N-2, 5:5:1 (*v*/*v*/*v*) were performed in the same manner as the calibration experiments (Figure S2). The starting Ca^{2+} concentration was $[Ca^{2+}] = 0.1359$ mM. The obtained results were an average of three titrations; determined slope: $S = 29.84$ mV.

Standard addition method: The same titrations with BEM were used to calculate the exact concentration of Ca^{2+} in the solution. A Gran plot of $10^{E/S}$ (S value from the calibration experiments) versus increase in concentration produced by each addition of the standard Ca^{2+} solution (C_s) was plotted, and the unknown concentration (C_u) was determined as the negative intercept on the x axis.[34] The average values of the determined concentrations were compared with the values of total Ca^{2+} concentration (Figure 4).

Acknowledgements

The authors thank T. Verbić, Dr. D. Linke, Prof. Dr. S. Petoud, Prof. Dr. H. A. Mayer and Prof. Dr. M. E. Maier for the helpful discussions and providing access to the NMR spectroscopy facilities. The financial support of the Max-Planck Society, the Hertie Foundation, the Louis-Jeantet Foundation, the Human Frontiers Science Program (long-term fellowship to S.C.) and the Centre National de la Recherche Scientifique (CNRS, France) is gratefully acknowledged. This work has been performed within the frame of the European COST Action D38 "Metal-Based Systems for Molecular Imaging Applications".

Keywords: calcium · gadolinium · imaging agents · magnetic resonance imaging

[1] N. K. Logothetis, *Nature* **2008**, *453*, 869–878.
[2] N. K. Logothetis, B. A. Wandell, *Annu. Rev. Physiol.* **2004**, *66*, 735–769.
[3] N. K. Logothetis, L. Pauls, M. Augath, T. Trinath, A. Oeltermann, *Nature* **2001**, *412*, 150–157.
[4] *The Chemistry of Contrast Agents in Magnetic Resonance Imaging* (Eds.: A. E. Merbach, E. Toth), Wiley, Chichester, **2001**.
[5] P. Caravan, J. J. Ellison, T. J. McMurry, R. B. Lauffer, *Chem. Rev.* **1999**, *99*, 2293–2352.
[6] A. Jasanoff, *Curr. Opin. Neurobiol.* **2007**, *17*, 593–600.
[7] S. Zhang, K. Wu, A. D. Sherry, *Angew. Chem.* **1999**, *111*, 3382–3384; *Angew. Chem. Int. Ed.* **1999**, *38*, 3192–3194.
[8] S. Aime, S. G. Crich, M. Botta, G. Giovenzana, G. Palmisano, M. Sisti, *Chem. Commun. (Cambridge)* **1999**, 1577–1578.
[9] S. Aime, D. D. Castelli, E. Terreno, *Angew. Chem.* **2002**, *114*, 4510–4512; *Angew. Chem. Int. Ed.* **2002**, *41*, 4334–4336.
[10] W-h. Li, S. E. Fraser, T. J. Meade, *J. Am. Chem. Soc.* **1999**, *121*, 1413–1414.
[11] T. Atanasijevic, M. Shusteff, P. Fam, A. Jasanoff, *Proc. Natl. Acad. Sci. USA* **2006**, *103*, 14707–14712.
[12] K. Hanaoka, K. Kikuchi, Y. Urano, T. Nagano, *J. Chem. Soc. Perkin Trans. 2* **2001**, 1840–1843.
[13] J. L. Major, G. Parigi, C. Luchinat, T. J. Meade, *Proc. Natl. Acad. Sci. USA* **2007**, *104*, 13881–13886.
[14] R. Trokowski, J. Ren, F. K. Kalman, A. D. Sherry, *Angew. Chem.* **2005**, *117*, 7080–7083; *Angew. Chem. Int. Ed.* **2005**, *44*, 6920–6923.
[15] V. Comblin, D. Gilsoul, M. Hermann, V. Humblet, V. Jacques, M. Mesbahi, C. Sauvage, J. F. Desreux, *Coord. Chem. Rev.* **1999**, *185–186*, 451–470.
[16] E. L. Que, C. J. Chang, *J. Am. Chem. Soc.* **2006**, *128*, 15942–15943.
[17] R. A. Moats, S. E. Fraser, T. J. Meade, *Angew. Chem.* **1997**, *109*, 749–752; *Angew. Chem. Int. Ed. Engl.* **1997**, *36*, 726–728.
[18] A. Y. Louie, M. M. Hüber, E. T. Ahrens, U. Rothbächer, R. Moats, R. E. Jacobs, S. E. Fraser, T. J. Meade, *Nat. Biotechnol.* **2000**, *18*, 321–325.
[19] A. L. Nivorozhkin, A. F. Kolodziej, P. Caravan, M. T. Greenfield, R. B. Lauffer, T. J. McMurry, *Angew. Chem.* **2001**, *113*, 2987–2990; *Angew. Chem. Int. Ed.* **2001**, *40*, 2903–2906.
[20] S. Aime, M. Botta, E. Gianolio, E. Terreno, *Angew. Chem.* **2000**, *112*, 763–766; *Angew. Chem. Int. Ed.* **2000**, *39*, 747–750.
[21] J. Waters, M. Larkum, B. Sakmann, F. Helmchen, *J. Neurosci.* **2003**, *23*, 8558–8567.
[22] J. N. D. Kerr, D. Greenberg, F. Helmchen, *Proc. Natl. Acad. Sci. USA* **2005**, *102*, 14063–14068.

[23] K. Ohki, S. Chung, Y. H. Ch'ng, P. Kara, R. C. Reid, *Nature* **2005**, *433*, 597–603.
[24] G. G. Somjen, *Ions in the Brain: Normal Function, Seizures, and Stroke*, Oxford University Press, New York, **2004**.
[25] M. G. Shapiro, T. Atanasijevic, H. Faas, G. G. Westmeyer, A. Jasanoff, *Magn. Reson. Imaging* **2006**, *24*, 449–462.
[26] C. Nicholson, G. ten Bruggencate, H. Stockle, R. Steinberg, *J. Neurophysiol.* **1978**, *41*, 1026–1039.
[27] The IUPAC Stability Constants Database, SC-Database, Academic Software and K. J. Powell, 1999, http://www.acadsoft.co.uk.
[28] K. Dhingra, P. Fousková, G. Angelovski, M. E. Maier, N. K. Logothetis, É. Tóth, *J. Biol. Inorg. Chem.* **2008**, *13*, 35–46.
[29] A. Mishra, P. Fousková, G. Angelovski, E. Balogh, A. K. Mishra, N. K. Logothetis, É. Tóth, *Inorg. Chem.* **2008**, *47*, 1370–1381.
[30] J. B. Livramento, C. Weidensteiner, M. I. M. Prata, P. R. Allegrini, C. F. G. C. Geraldes, L. Helm, R. Kneuer, A. E. Merbach, A. C. Santos, P. Schmidt, E. Toth, *Contrast Media Mol. Imaging* **2006**, *1*, 30–39.
[31] S. Canals, M. J. Casarejos, S. de Bernardo , E. Rodriguez-Martin, M. A. Mena, *J. Neurochem.* **2001**, *79*, 1183–1195.
[32] M. Giardiello, M. P. Lowe, M. Botta, *Chem. Commun. (Cambridge)* **2007**, 4044–4046.
[33] J. I. Bruce, R. S. Dickins, L. J. Govenlock, T. Gunnlaugsson, S. Lopinski, M. P. Lowe, D. Parker, R. D. Peacock, J. J. B. Perry, S. Aime, M. Botta, *J. Am. Chem. Soc.* **2000**, *122*, 9674–9684.
[34] B. R. Eggins, *Chemical Sensors and Biosensors*, Wiley, Chichester, **2002**.
[35] D. M. Corsi, C. Platas-Iglesias, H. van Bekkum, J. A. Peters, *Magn. Reson. Chem.* **2001**, *39*, 723–726.
[36] A. Beeby, I. M. Clarkson, R. S. Dickins, S. Faulkner, D. Parker, L. Royle, A. S. de Sousa, J. A. G. Williams, M. Woods, *J. Chem. Soc. Perkin. Trans. 2* **1999**, 493–503.

Received: March 17, 2008
Published online on July 4, 2008

